

Disturbance Modeling, Simulation and Testing of Solar Array Drive Assembly

Xue Li¹, Wei Cheng¹ and Wei Han²

¹*School of Aeronautical Science and Engineering, Beihang University,
NO.37, Xueyuan Road, Beijing 100191, China*

²*China Aero-Polytechnology Establishment, No.7, Jingshun Road, Chaoyang District,
Beijing, 100028, China*

¹*daxue129.student@sina.com, ²cheng_wei@buaa.edu.cn*

Abstract

Solar panel is an important structure of the spacecraft, SADA (Solar Array Drive Assembly) is often used as the drive organ to realize the step-skipped gesture adjustment. Firstly, the disturbance mechanism impact, which was produced from working SADA, to the electro-mechanism and payload coupling has been taken into account, and the dead, rigid and flexible load SADA disturbance model was established and validated through simulation and experimental measuring. Secondly, implemented the experimental check, calibration and correction to the mathematical model. Finally, the definition of electrical rigidity was proposed to analyze the disturbance mechanism of SADA, and verified its existence through simulation and testing.

Key words: *stepper motor, mechanics-electricity coupling, load, disturbance*

1. Introduction

One of the factors that may impact the directional accuracy, imaging quality and other crucial functions of the high-precise spacecraft is the micro-vibration of itself. There are many possible sources of such disturbance, as the momentum wheel, CMG, SADA, satellite antenna, etc.

The SADA drives the solar panel to trace the source of solar radiation corresponding to spacecraft's rotation. For features of highly accurate positioning, non-cumulative error, excellent stability of average speed under long-term operation, simple driver circuit and easy open-loop control of the stepper motor, SADA was widely implemented. The study of the SADA instruments plays an important role in understanding the impact to the spacecraft's attitude stability produced by solar panel rotation and strengthening the directional accuracy and camera imaging quality of spacecrafts by implementing corresponding isolating and controlling technologies.

In recent years, there are a great number of references aiming at illustrating the operational principle of the two-phase hybrid stepper motor and the micro-step controlling driving principle [1-5,10-13,16-19], designing the micro-step controlling driver circuit [6], and studying the stepper motor's speed control mechanism [7]. Meng Zhang from Beijing Institute of Control Engineering, for instance, proposes a controlling method of torque compensation to enhance the stability of SADA's operation speed [8]. Zhu Si-hua has designed the self-adaptation current compensation driver to neutralize the impact of friction torque of driving instrument and driving torque, and then improved the accuracy and stability

of spacecraft attitude control [9]. However, most of their works is based only on the modeling and simulation, and there are few researches on the disturbance and load feature of SADA conducted by experimentation.

In this paper, the disturbing force generated from the stepper motor and the solar panel's intrinsic mode is fully considered and the mathematical model of the spacecraft disturbance brought by flexible load electro-mechanical system is established. Through MATLAB simulation and the designation of an experiment to verify the simulation result, the model is validated with substantial proof. While analyzing the SADA disturbing mechanism, the definition of electromagnetic rigidity is raised, and its existence is verified by the experiment. Generally speaking, this paper can be implemented to evaluate the imaging quality of the spacecraft camera, and provide substantial reference to related studies.

2. Analysis of the Principle of Solar Panel Driving Mechanism

The driving function of a solar panel is provided by the stepper motor. When the stepper motor driver receives an electrical pulse, it rotates for a specific stepper angular towards a predefined direction. A specific angular displacement thus will be achieved by controlling the number of pulses. The motor rotation speed and acceleration will be the same as the pulse frequency [14].

The teeth number of the motor used in the experiment is Z , operating beats number p . The relation between stepper angular θ and beats number is

$$\theta = \frac{360^\circ}{Z \times p} \quad (1)$$

Due to the limitation of manufacturing technique, the stepper angular is generally larger than expected, along with lower vibration frequency. By implementing a normal driving mechanism, the amplitude produced by the stepper angular is also larger. As a result, it could be quite possible to lose steps in this procedure. Current control and subdivision driving technologies would be implemented in this paper to raise the controlling precision, and achieve the subdivision stepper angular through controlling the current of each phase's winding coil to transfer the sine (cosine) current to trapezoidal wave that changes according to the sine (cosine) function.

The subdivision number of stepper is n , and then the motor shaft angular of each step should be:

$$\phi = \frac{\theta}{n} \quad (2)$$

3. Modeling of SADA Disturbance

3.1. The principles of producing SADA disturbance and electromagnetic rigidity

Disturbance model is the mathematical induction model for the disturbing mechanic nature of disturbing source. The stepper is the most significant feature of the SADA. Stepper motor is an electro-mechanical apparatus driven by electrical pulses. The resonance amplitude corresponding to each single step is directly related to the increment of each step. Besides, normal driving method would generate larger amplitude for bigger step distance. Within the system's natural resonance region, it would be quite possible to lose steps. To divide one

natural step of the motor into micro-subdivisions would significantly enhance the resolution of the former problem. Due to the smaller step distance, stabler motor operation, smaller amplitude and lower noise features of the micro stepper motor, there could be fewer lost steps even when it is still in the resonance region. The SADA with micro subdivision has two fundamental frequencies:

$$f_1 = \frac{v}{\theta} \quad \text{and} \quad f_2 = \frac{v}{\phi} \quad (3)$$

The magnetic field synthesis direction inside the motor would be modified to drive the motor rotating by electrifying the 2 phase winding coil in turn. Along with the incoming pulses, the rotor moves relatively to the stator in steps. Theoretically, one pulse would drive the rotor to rotate in a certain angular γ to get an equilibrium position. Nonetheless, for the sake of electromagnetic rigidity, the rotor is not staying in stationary when it just finishes the last step and waits for the next one. In reality, it is staying in resonance region with an amplitude $\Delta\theta$ around the equilibrium position.

To study the overall disturbance feature of solar panel driven by SADA by means of simulation and experimentation, three models would be implemented. 1) Dead load SADA model, to calculate the disturbance feature of itself; 2) Rigid load SADA model, to calculate its electromagnetic and rigid coupling feature; 3) Flexible load SADA model, to illustrate the exact disturbance feature of SADA driven solar panel.

3.2. Dead load SADA model

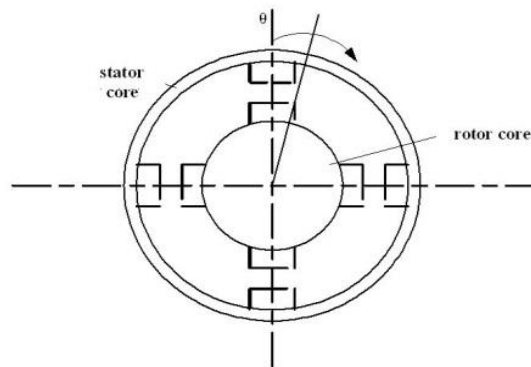


Figure 1. Model of stepper motor

$$J \ddot{\theta} = T_e - M_d \quad (4)$$

T_e and M_d respectively are the driving torque and damping torque applied from stator to rotor; J is the rotary inertia of the stepper rotor; θ is the angular acceleration of the stepper rotor.

3.3. Rigid load SADA model

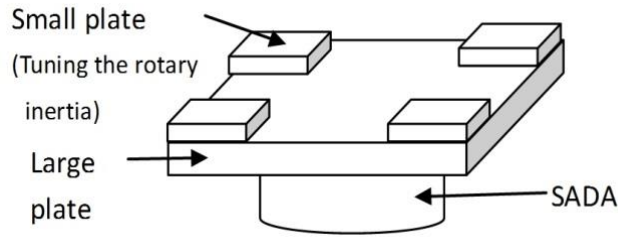


Figure 2. Rigid load SADA model

The mathematical model of rigid load SADA would also include torque equation, voltage equation and disturbance equation. These equations are the bases of stepper motor control.

The disturbance equation of moving rotor consists of driving torque and damping torque:

$$(J + J_1)\ddot{\theta} = T_e - M_d \quad (5)$$

In this equation, J_1 is the rotary inertia of rigid load, and J is negligibly small compared to J_1 .

3.4. Flexible load SADA model

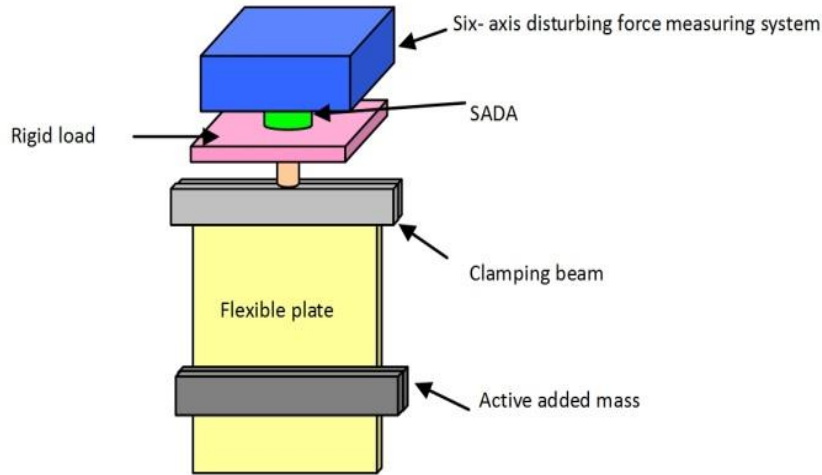


Figure 3. Flexible load SADA model

Consider only the elastic and rigid model inertia coupling, the flexible load SADA model could be:

$$\begin{bmatrix} J_1 & 0 \\ 0 & J_2 \end{bmatrix} \begin{bmatrix} \ddot{\theta} \\ \ddot{\phi} \end{bmatrix} + \begin{bmatrix} B + c_2 & -c_2 \\ -c_2 & c_2 \end{bmatrix} \begin{bmatrix} \dot{\theta} \\ \dot{\phi} \end{bmatrix} + \begin{bmatrix} k_1 & k_2 \\ -k_2 & k_2 \end{bmatrix} \begin{bmatrix} \theta \\ \phi \end{bmatrix} = \begin{bmatrix} T_e \\ 0 \end{bmatrix} \quad (6)$$

J_1 is the rotary inertia (Due to the momentum inertia is quite small, the major rotary inertia would be produced from rigid load and clamping beam); J_2 is the flexible load

SADA's rotary inertia; B is the torsional damping of SADA; C_2 is the torsional damping of flexible load SADA; $k_1 = k_d$ is the electromagnetic rigidity; k_2 is the torsional rigidity of flexible load; T_e is the output torque of the motor; θ is the SADA output rotor angle; ϕ is the flexible load rotor angle.

Above is the disturbance model of SADA, which considers the varying pattern of its amplitude corresponding with time. The disturbance model could be interpreted into a group of overlapping simple harmonic waves. Except for the frequency of each harmonic wave, there is frequency multiplication. Therefore the disturbance model of SADA should be:

$$m(t) = \sum_{i=1}^n C_i T_e \sin(n\alpha_i \omega t + \alpha_i) \quad (7)$$

Where, $m(t)$ is the disturbance, and it could be either force or torque; n is the number of simple harmonic force; C_i is the coefficient of number i harmonic force amplitude, it would be calculated from the experiment; f_i is the frequency of the number i harmonic, corresponding to the f_1 and f_2 's frequency multiplication in (3); α_i is the phase of the number i harmonic force; T_e is the motor torque which is a quite important parameter for the electromagnetic rigidity.

4. SADA Simulation and Validation

The mathematical model of stepper motor consists of torque, physical and motion equations. Those equations are the fundamental principles of stepper motor control [16]. The math model of two phase hybrid stepper motor is:

$$\text{Electrical: } \begin{cases} T_e = p \left[L_2 (I_A^2 - I_B^2) \sin(2p\theta) - 2I_A I_B L_2 \cos(2p\theta) \right] \\ \quad + K_t [I_B \cos(p\theta) - I_A \sin(p\theta)] - D \sin(4p\theta) \\ M_d = B \dot{\theta} \end{cases} \quad (8)$$

$$\text{Electromagnetic: } \begin{cases} U_a = I_a R + L \frac{dI_a}{dt} - K_e \dot{\theta} \sin(p\theta) \\ U_b = I_b R + L \frac{dI_b}{dt} + K_e \dot{\theta} \cos(p\theta) \end{cases} \quad (9)$$

For the parameters in the above model: p - Teeth number of the rotor; L_2 -coefficient of mutual inductance; K_t -Coefficient of torque; K_e -Coefficient of anti-electromotive force; θ -Angular displacement of the rotor; R -Resistance; L - Self-induction coefficient; J_1 -Rotary inertia of motor shaft; B -Coefficient of viscous friction; I_A and I_B -Current of two-side winding coil; U_a and U_b -Voltage of two-phase winding coil; D -Coefficient of positioning torque. Because of the difficulty of direct testing, some of the parameters value will be cited from outer resources together with estimation test, and some just use the values provided by motor manufacturer. Nevertheless, all the parameter values would be displayed in international standard unit system.

To implement the Simulink simulation based on the stepper math model, the principle of the simulation is:

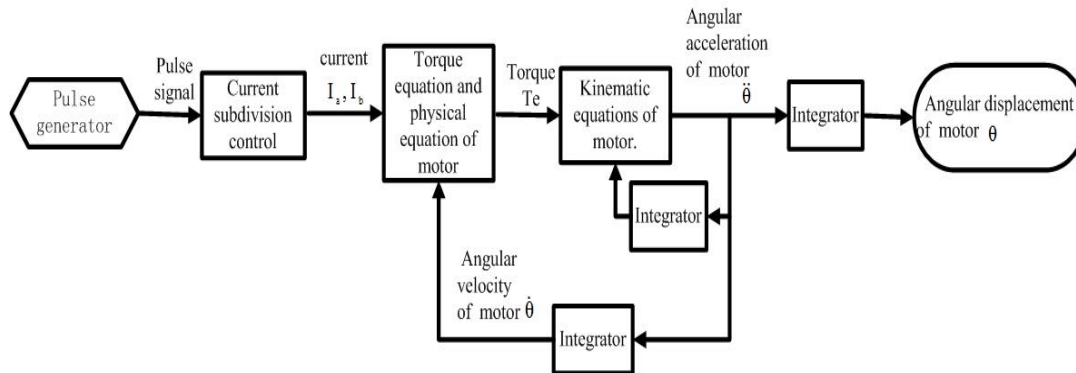


Figure 4. Simulation principle of stepper motor

The input signal of stepper motor is periodical electrical pulses. I_a and I_b is the sine-wave current with a phase difference $\pi/2$ generated from the current subdividing device, then use tuned current as the input of the motor and harmonic reducer math model, and the result is mechanical angular displacement θ , and disturbance torque T of the antenna. The simulated motor current I_a, I_b and stepper motor acceleration $\ddot{\theta} = d^2\theta/dt^2$ could be calculated from the simulation.

To simulate the stepper motor's math model by using the rotation speed $v = 0.058^\circ/s$, and from (3) we could get two base frequencies of the motor: $f_1 = 0.193\text{Hz}$ and $f_2 = 49.5\text{Hz}$. The simulated current, angular acceleration, and angular are shown in the below graph:

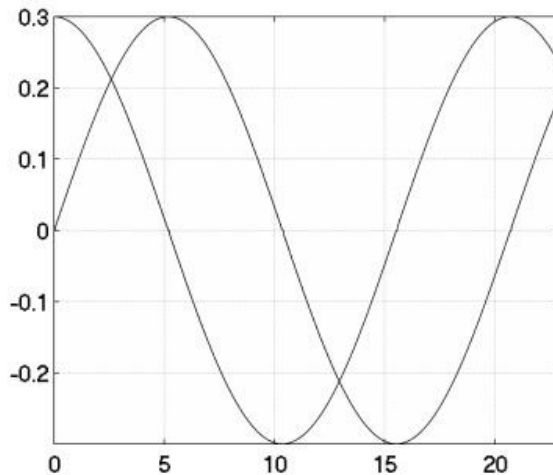


Figure 5. Simulated current for stepper motor

In Figure 5, the discretization sine-wave of simulated current with the amplitude 0.3A is subdivided into 256 steps in 1/4 cycles. After the subdivision, the pulse cycle is 0.0202s with corresponding frequency 49.5Hz. 1/4 sine-waved current cycle is 5.175s with corresponding frequency 0.193Hz.

To simulate SADA model under dead load, rigid load and flexible load, only the angular acceleration frequency domain graph of rigid load is provided, and the rigid load is: $0.2045 \text{ kg}\cdot\text{m}^2$, $0.3237 \text{ kg}\cdot\text{m}^2$, $0.4430 \text{ kg}\cdot\text{m}^2$. The frequency brought by electromagnetic rigidity is defined as electromagnetic frequency f_d , and corresponding acceleration $\ddot{\theta}_d$.

The rotation speed is $v = 0.058^\circ / s$, rigid load is $0.3237 \text{ kg}\cdot\text{m}^2$, $f_d = 9.9 \text{ Hz}$ with the angular acceleration $\ddot{\theta}_d = 2.4 \cdot 10^{-3} \text{ rad} / s^2$. The simulation of rotary torque and angular acceleration is shown in the following graph:

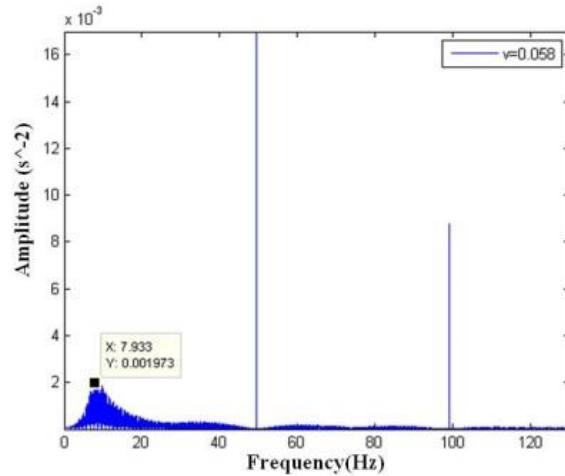


Figure 6. Frequency domain graph of SADA angular acceleration

From the above graph, we could recognize that the electromagnetic frequency is 7.933Hz, subdivision of the stepper motor current is 49.5Hz and its 2 frequency multiplication.

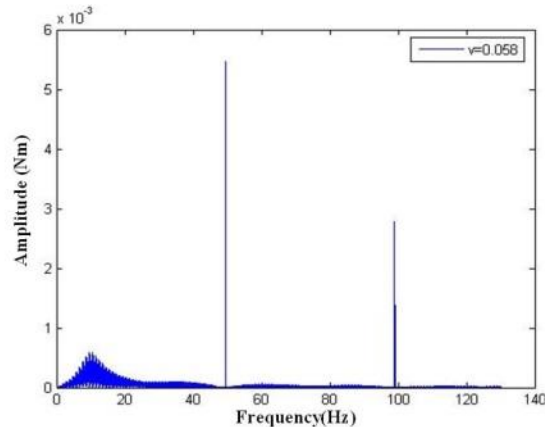


Figure 7. Output torque of SADA

Figure 7 is the simulated frequency domain graph of rotary torque, and its disturbance frequency is the same as the electromagnetic frequency, current incentive frequency and the double frequency multiplication.

It is demonstrated in Figure 8 that the simulated SADA revolves 0.01 radian in 10s and the angular speed is steadily $0.058^\circ/s$, so that the validation of the simulation model was proved. (see the simulation graph for detailed information below):

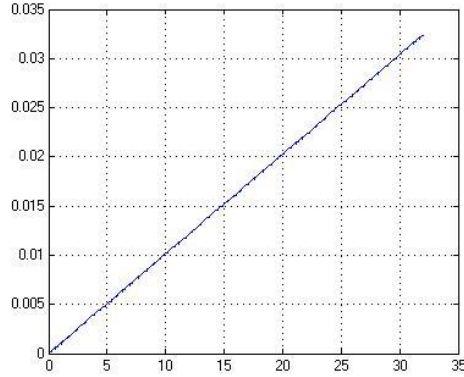


Figure 8. Simulation angle curve under rotation speed $\nu = 0.058^\circ/s$

The simulation result of angular acceleration and torque of flexible coupling load SADA is shown in the following table:

Table 1. Simulation results of angular acceleration and torque of flexible coupling load SADA under different rotary speed

Rotary speed (rad/s)	Frequency(Hz)	Angular acceleration(rad/s ²)	Torque(N•m)
0.058	2.5	0.81	2.3
	6.06	37.8	20.7
	49	7.9	4.52
0.063	2.5	0.86	2.55
	6.06	63.8	34.9
	53.8	9.1	5.15
0.0715	2.5	0.64	1.98
	6.06	33.7	18.4
	61	9.1	5.22
0.6	2	4.82	4.2
	2.5	4.62	4.3
	6.6	211	115

5. SADA Disturbance Measuring Experiment

5.1. Dead load SADA experiment

Test the current and angular acceleration of dead load SADA using rigid six-axis testing table. The frequency of the testing table is above 700Hz. The motor is installed inside the testing table. Measure the tangential acceleration of the hybrid stepper motor with the

acceleration sensors, and calculate the working motor angular acceleration with the equation $\alpha = a / r$. The testing current is shown in the following graphs:

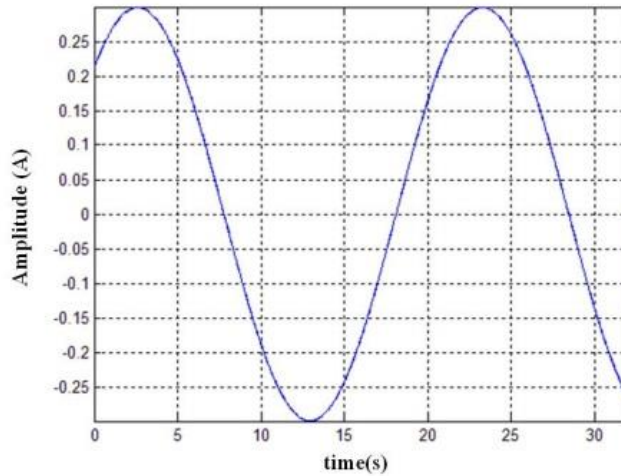


Figure 9. Dead load testing current

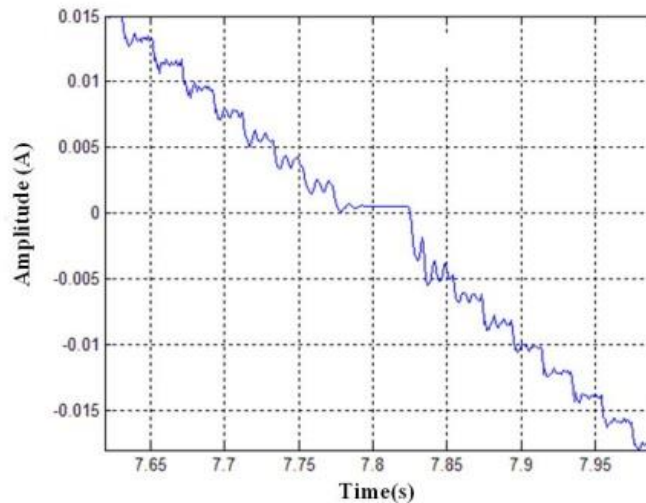


Figure 10. Magnification of partial current curve

We could see that the current measured in the experiment was not the same as simulation, which conformed to a sort of oscillation at every phase. But it would not affect the angular acceleration feature of the stepper motor. Due to the accuracy of the current subdivision device, the stepper could be approximately 3 times bigger than usual when crossing the zero point. In the meantime, the angular acceleration could attenuate when the electromagnetic torque was weakening. All these would exert impact on the disturbance feature of SADA. Meanwhile, the changes of current amplitude would result in a relatively big angular acceleration oscillation, which means that each step of the working motor would make a significant oscillation of itself.

The dead load experiment of the SADA could calculate the number of current subdivisions

and validate the mathematical model of SADA (Torsional torque equation, physical equation and motional equations). The base frequencies of both experimental and simulation include 49.5Hz and 0.193Hz, consistent with the theoretical value.

5.2. Rigid load SADA experiment

The experiment method is driving three loads SADA directly with different rotary inertia and analyzing the SADA disturbance feature by measuring the testing current, angular acceleration and disturbance. The rotary inertia could be tuned by eight square metal plates.



Figure 11. SADA with rigid load

When the rotary speed of SADA was $\dot{\theta}=0.058^\circ / s$ and rotary inertia was $0.3237 \text{ kg}\cdot\text{m}^2$, the frequency domain (within 140Hz) of angular acceleration and torque had three frequencies: electromagnetic frequency, current excitation frequency and the double frequency.

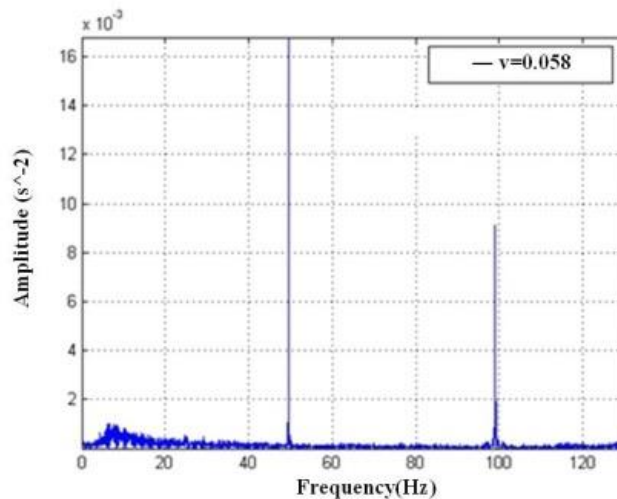


Figure 12. SADA angular acceleration frequency domain graph

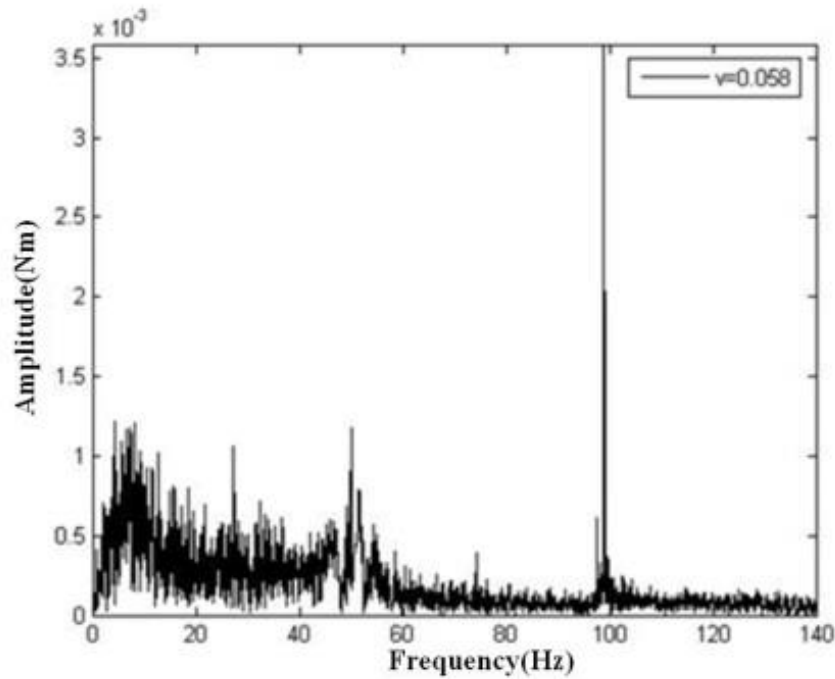


Figure 13. SADA output torque

Though the noises of bending moment measured in the experiment were larger than expected, it still could be considered as consistent with the simulated SADA torque frequency domain.

Table 2. Comparison of the experimental and simulated electromagnetic frequency

Torsional inertia	Electromagnetic Frequency (Simulation)	Electromagnetic Frequency (Experimental)	Frequency error (%)
0.2045	9.9	9.59	3.23
0.3237	7.867	7.63	3.07
0.4430	6.733	6.51	3.37

The current excitement frequency is relevant to the rotary speed instead of the load. The amplitude of angular acceleration and torque at the electromagnetic frequency would decrease along with the increasing rotary inertia, but rise with the increasing rotary speed.

$$f_d = \frac{1}{2\pi} \sqrt{\frac{k_d}{J}} \quad (10)$$

According to the angular acceleration and torque frequency domain graph produced from the simulation and experiment, the electromagnetic frequency f_d could be identified to calculate the SADA electromagnetic rigidity. From Table 2, it could be concluded that the simulation were consistent with experimental results. The electromagnetic rigidity would exert certain impact to the natural frequency of the payload, just like a torsional spring

mounted between the motor and payload. When the natural frequency of the payload became close to the natural frequency of the entire structure, which consisted of the engine bedplate, motor and payload, great structural vibration generated from the resonance would lower the controlling precision of the whole system.

5.3. Flexible load SADA experiment



Figure 14. Flexible load SADA experiment

In the flexible load SADA experiment, moving the rigid clamping plate vertically until its distance towards the aluminum plate was approximately 20cm, and then the overall state would be the best (see above picture for more details). The nature frequency of the load was: first order bending frequency 2.344Hz and first order torsional frequency 2.563Hz.

The disturbance frequency calculated in the experiment was 49.5Hz with the amplitude $0.03264 N \cdot m$ (see the below graph). When the rotary speed was $0.058^\circ / s$, the disturbance testing result could be seen from the Figure 16 below.

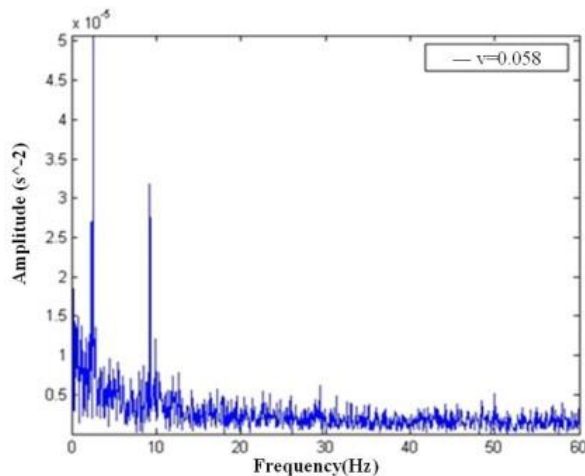


Figure 15. Flexible SADA angular acceleration frequency domains

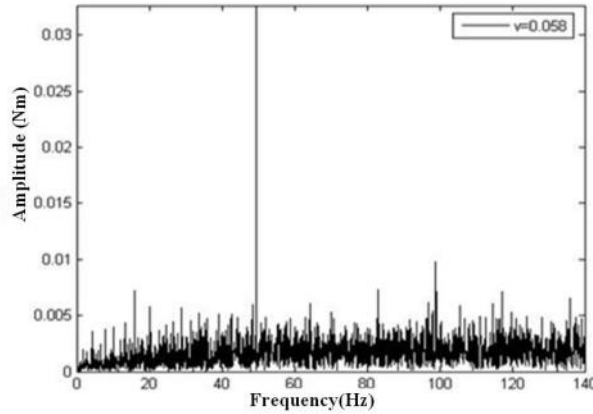


Figure 16. SADA output torque

With the SADA working at the speed of 0.058°/s, the acceleration sensor was mounting on the flexible plate. From Figure 15, we could tell that only two frequencies could be measured within 60Hz, 2.5Hz and 9.25Hz, while, the current excitement frequency 49.5Hz is missing. Around the 9.25Hz, there was a disturbance frequency which could be verified as environmental noises through measuring when SADA was not working. Due to the large damping generated from the sensor position, the weakened amplitude of electromagnetic frequency produced by electromagnetic rigidity could not be measured from this experiment. Therefore, only the frequency of coupled flexible load could be measured. The measurement of flexible load SADA torque under different rotary speed was provided in Table 3.

Table 3. Flexible load SADA rotary disturbance under different rotary speed

Rotary speed(rad/s)	Rotary frequency(Hz)	Torque amplitude(N•m)
0.058	49.5	0.03264
0.063	53.75	0.03063
0.0715	61.06	0.01928
0.6	2	0.001018

From the above table, we could conclude that the frequency calculated in the experiment is consistent to the theoretical value, whereas the amplitude would be smaller due to the significant damping of flexible plate.

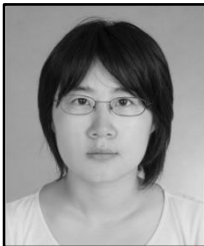
6. Conclusion

- (1) We have successfully built the disturbance model for loaded operating stepper motor and precisely illustrate the active features of SADA driven load in this research.
- (2) Through theoretical analysis, simulation, and experimental comparison, the existence of electromagnetic rigidity could be proved and accurately measured.
- (3) We built the mathematic model of disturbance force exerted from flexible load stepper motor mechanism to the spacecraft and verified the simulation through the experiment result. Thus a substantial reference to other motion parts mounted on the spacecraft was provided.

References

- [1] J. -L. Li, "Design of Two-phase Hybrid Stepping Motor Subdivision Driver IC Based on PWM", Xi'an University of Science and Technology, (2005).
- [2] S. -Y. Zhang and X. -M. Wang, "Study of Fuzzy-PID Control in MATLAB for Two-phase Hybrid Stepping Motor", Proceedings of the 2nd International Conference On Systems Engineering and Modeling (ICSEM-13).
- [3] L. Andres and S. Jorge, "Speed Estimation of PM Stepper Motors. Robustness Aspects", Power Electronics and Motion Control Conference 2006, EPE-PEMC 2006, 12th International, (2006) August 30-September 1, pp. 1121-1126.
- [4] H. Melkote and F. Khorrami, "Adaptive Variable Structure Torque Ripple Cancellation for Permanent Magnet Stepper Motors", Proceedings of the 1998 American Control Conference, vol. 2, (1998), June 24-26, pp. 1033-1037.
- [5] H. Melkote and F. Khorrami, "Robust Nonlinear Control and Torque Ripple Reduction for Permanent Magnet Stepper Motors", Control Theory and Applications, IEEE Proceedings, vol. 146, Issue 2, (1999) March, pp. 186-196.
- [6] Z. -Y Xu, Z. -J. Wen and W. -H. Chen, "Design of Two-phase Microstepping Driver Based on FPGA", Electric Drive, vol. 38, no. 4, (2008), pp. 59-62.
- [7] Y. -D. Liu, C. -X. Li and X. -X. Wang, "Precise Control of Step Motor Speed", Journal of Shanghai, Jiaotong University, vol. 10, no. 35, (2001), pp. 1517-1520.
- [8] M. Zhang, L. -X. Zhu and J. Lu, "A High Stability Control Method for Solar Array Drive Mechanism", Aerospace Control and Application, no. 08, (2010), pp. 2-5.
- [9] S. -H. Zhu, Y. -W. Liu and K. Li, "Research on Modeling and Driver Design of Solar Array Drive Assembly", Aerospace Control and Application, vol. 36, no. 2, (2010), pp. 5-10.
- [10] D. Brandel, "The advanced tracking and data relay satellite system (ATDRSS)", The next generation, AAS, (1988), pp. 263-269.
- [11] M. -W. Zhou, "Modeling and Control of the Satellite with Dual Axis Solar Array Actuator", Harbin Institute of Technology, vol. 7, no. 4, (2010), pp. 5-10.
- [12] J. -Y. Liu, "Modeling Method of Rigid-Flexible Coupling", Shanghai JiaoTong University, (2000).
- [13] H. Melkote and F. Khorrami, "Robust Nonlinear Control and Torque Ripple Reduction for Permanent Magnet Stepper Motors", Control Theory and Applications, IEEE Proceedings, vol. 146, Issue 2, (1999) March, pp. 186-196.
- [14] Z. -Y. Shu, J. -L. Liu and X. -X. Zhang, "Research of Multi-Degree-of-Freedom Stepper Motor Drive System", Small & Special Electrical Machines, vol. 41, no. 1, (2013).
- [15] X. -F. Wang, "Disquisition of stepper motor subdivision driving", Journal of JngGangShan University (NATURAL SCIENCES), vol. 28, no. 5, (2007).
- [16] Y. Liu, C. Li and X. Wang, "Precisecontrol of step motor speed, Journal of Shanghai Jiaotong University, vol. 10, no. 35, (2001), pp. 1517-1520.
- [17] T. Burg, J. Hu, D. Dawson and P. Vedagarbha, "A global exponential position tracking controller for a permanent magnet stepper motor via output feedback", Proceedings of the Third IEEE Conference on Control Applications, vol. 1, (1994) August 24-26, pp. 213-220, DOI: 10.1109/CCA.
- [18] S. Kamalasan, "A New Intelligent Controller for the Precision Tracking of Permanent Magnet Stepper Motor", Power Engineering Society General Meeting, (2007) June, 24-28, IEEE, pp. 1-7.
- [19] M. Bodson, J. S. Sato and S. R. Silver, "Spontaneous speed reversals in stepper motors", Decision and Control, 2003, Proceedings, 42nd IEEE Conference, vol. 4, (2003) December 9-12, pp. 3319 - 3324

Authors



Xue Li

She is a Ph.D. candidate in Beihang University, Beijing, 100191, China. Her main research interest is micro-vibration analysis and control on spacecraft now.



Wei Cheng

He is a professor and a Ph.D. supervisor in Beihang University, Beijing, 100191, China. His main research interests are structural dynamics and vibration control.



Wei Han

He is an assistant engineer. He graduated from Beihang University in January 2013. His main research directions are structural dynamics, virtual vibration test and environmental test technology.

